

Neutron Star Crust in Strong Magnetic Fields

Rana Nandi and Debades Bandyopadhyay

Astroparticle Physics and Cosmology Division, Saha Institute of Nuclear Physics, 1/AF
Bidhannagar, Kolkata-700064, India

E-mail: debades.bandyopadhyay@saha.ac.in

Abstract. We discuss the effects of strong magnetic fields through Landau quantization of electrons on the structure and stability of nuclei in neutron star crust. In strong magnetic fields, this leads to the enhancement of the electron number density with respect to the zero field case. We obtain the sequence of equilibrium nuclei of the outer crust in the presence of strong magnetic fields adopting most recent versions of the experimental and theoretical nuclear mass tables. For $B \sim 10^{16}$ G, it is found that some new nuclei appear in the sequence and some nuclei disappear from the sequence compared with the zero field case.

Further we investigate the stability of nuclei in the inner crust in the presence of strong magnetic fields using the Thomas-Fermi model. The coexistence of two phases of nuclear matter - liquid and gas, is considered in this case. The proton number density is significantly enhanced in strong magnetic fields $B \sim 10^{17}$ G through the charge neutrality. We find nuclei with larger mass number in the presence of strong magnetic fields than those of the zero field. These results might have important implications for the transport properties of the crust in magnetars.

1. Introduction

The discovery of a new class of neutron stars with very strong magnetic fields called magnetars has greatly enhanced the interest in the study of neutron star properties in the presence of strong magnetic fields [1]. Their surface magnetic fields could be $\geq 10^{15}$, as predicted by observations on soft gamma-ray repeaters and anomalous x-ray pulsars [2, 3]. Such strong magnetic fields might be generated by dynamo processes in newly born neutron star [4]. In the core region the magnetic field may be even higher, the limiting value (B_{max}) is obtained by the scalar virial theorem [5]. For a typical neutron star ($M = 1.5M_{\odot}$, $R = 15$ km) this value is $B_{max} \sim 10^{18}$ G. Such high magnetic fields can have significant effects on the equilibrium nuclear composition and equation of state in neutron star crust and interior [5, 6].

Nonmagnetic equilibrium composition and equation of state for the outer crust was reported in a seminal paper by Baym, Pethick and Sutherland (BPS) [7]. Outer crust contains nuclei arranged in a body-centered (bcc) lattice immersed in a gas of free electrons which are relativistic above the density $\rho \sim 10^7$ g cm $^{-3}$. Though the lattice effect is small on the equation of state, it changes the equilibrium nucleus to a heavier one and lowers the total energy of the system by reducing the coulomb energy of the nucleus. At $\rho \sim 10^4$ g cm $^{-3}$, ^{56}Fe is present as the equilibrium nucleus, but with increasing density equilibrium nuclei become more and more neutron rich through electron capture process. At a density $\rho \simeq 4 \times 10^{11}$ g cm $^{-3}$ neutrons begin to drip out of nuclei - this is called neutron drip point. The inner crust begins from here. In the inner crust nuclei are immersed in a neutron gas as well as a uniform background of electrons.

Nuclei are also arranged in a lattice in the inner crust. The composition and the equation of state of the inner crust were earlier calculated by different groups [8, 9].

The composition and equation of state of the outer crust of nonaccreting cold neutron stars in the presence of strong magnetic fields were first studied by Lai and Shapiro [5]. In the presence of a magnetic field the motion of electrons perpendicular to the field get quantized into Landau orbitals. This causes the electron density to change which in turn modifies the coulomb energy. If the magnetic field is very strong then electrons occupy only the low-lying Landau levels and it may affect the sequence of nuclei and the equation of state as well as any nonequilibrium β -processes [5]. However, there is no calculation of the inner crust composition and equation of state in the presence of magnetic fields.

This paper is organised in the following way. We revisit the magnetic BPS [5] adopting recent experimental and theoretical nuclear mass tables in Section II. The inner crust in strong magnetic fields is discussed in Section III. We conclude in Section IV.

2. Magnetic BPS Model

We revisit the BPS model to find the sequence of equilibrium nuclei and calculate the equation state of the outer crust in the presence of strong magnetic fields $B \sim 10^{16}$ G [5]. In this calculation, we include the finite size effect in the lattice energy and adopt recent experimental and theoretical mass tables. Nuclei are arranged in a bcc lattice in the outer crust. The Wigner-Seitz (WS) approximation is adopted in this calculation. Each lattice volume is replaced by a spherical cell and contains one nucleus at the center. Each cell is taken to be charge neutral such that Z number of electrons presents in it, where Z is the nuclear charge. The Coulomb interaction between cells is neglected. To find an equilibrium nucleus (A, Z) at a given pressure P one has to minimize the Gibbs free energy per nucleon with respect to A and Z . The total energy density is given by

$$E_{tot} = n_N(W_N + W_L) + \varepsilon_e(n_e). \quad (1)$$

The energy of the nucleus (including rest mass energy of nucleons) is

$$W_N = m_n(A - Z) + m_p Z - bA, \quad (2)$$

where b is the binding energy per nucleon. Experimental nuclear masses are obtained from the atomic mass table compiled by Audi, Wapstra and Thibault (2003) [10]. For the rest of nuclei we use the theoretical extrapolation of Möller et al (1995) [11]. W_L is the lattice energy of the cell and is given by

$$W_L = -\frac{9}{10} \frac{Z^2 e^2}{r_C} \left(1 - \frac{5}{9} \left(\frac{r_N}{r_C} \right)^2 \right). \quad (3)$$

Here r_C is the cell radius and $r_N \simeq r_0 A^{1/3}$ ($r_0 \simeq 1.16$ fm) is the nuclear radius. The first term in W_L is the lattice energy for point nuclei and the second term is the correction due to the finite size of the nucleus (assuming a uniform proton charge distribution in the nucleus). Further ε_e is the electron energy density and P is the total pressure given by

$$P = P_e + \frac{1}{3} W_L n_N. \quad (4)$$

The nucleon number density n_N is related to the baryon number density n_b as

$$n_b = A n_N, \quad (5)$$

and the charge neutrality condition gives

$$n_e = Z n_N. \quad (6)$$

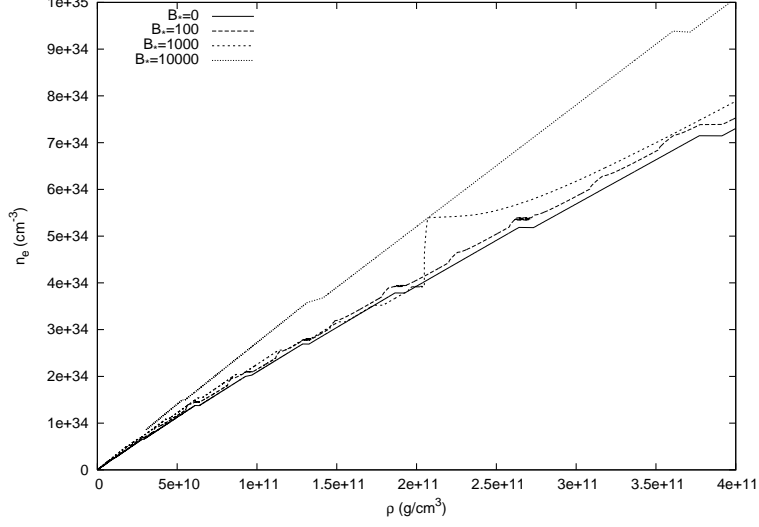


Figure 1. Electron number density is plotted with mass density for different magnetic field strengths.

In the presence of a magnetic field, the electron motion is Landau quantized in the plane perpendicular to the field. We take the magnetic field (\vec{B}) along Z-direction and assume that it is uniform throughout the outer crust. If the field strength exceeds a critical value $B_c = m_e^2/e \simeq 4.414 \times 10^{13}$ G, then electrons become relativistic. The energy eigenvalue of relativistic electrons in a quantizing magnetic field is given by

$$E_e(\nu, p_z) = \left[p_z^2 + m_e^2(1 + 2\nu B_*) \right]^{1/2}, \quad (7)$$

where p_z is the Z-component of momentum, $B_* = B/B_c$, and ν is the Landau quantum number.

The number density of electrons in a magnetic field is calculated as

$$n_e = \frac{eB}{2\pi^2} \sum_0^{\nu_{max}} g_\nu p_{f_e}(\nu), \quad (8)$$

where the spin degeneracy $g_\nu = 1$ for $\nu = 0$ and $g_\nu = 2$ for all other Landau levels. The maximum Landau quantum number ν_{max} is given by

$$\nu_{max} = \frac{\mu_e^2 - m_e^2}{2eB}, \quad (9)$$

where μ_e is the electron chemical potential. Energy density of electrons is given by,

$$\varepsilon_e = \frac{eB}{2\pi^2} \sum_0^{\nu_{max}} g_\nu \int_0^{p_{f_e}(\nu)} E_e(\nu, p_z) dp_z, \quad (10)$$

and the pressure of the electron gas is

$$P_e = \mu_e n_e - \varepsilon_e. \quad (11)$$

At a fixed pressure P , we minimize the Gibbs free energy per nucleon

$$g = \frac{E_{tot} + P}{n_b} = \frac{W_N + 4/3W_L + Z\mu_e}{A}, \quad (12)$$

varying A and Z of a nucleus.

Now we present our results for several values of magnetic fields $B_* = B/B_c = 0, 100, 1000$ and 10000 where $B_c = 4.414 \times 10^{13}$ G. In Fig. 1, electron number density is plotted with mass density for the above mentioned values of magnetic fields. For $B_* < 1000$, large numbers of Landau levels are populated. Consequently there is no significant change in the electron number density compared with that of the field free case. But there is a jump in the electron number density for $B_* = 10^3$ case when only zeroth Landau level is populated at $\sim 2 \times 10^{11}$ g/cm³. On the other hand, for $B_* = 10^4$, only zeroth Landau level is populated over the whole mass density range. In this case, the phase space modification due to the Landau quantization leads to the strong enhancement of electron number density with respect to the zero field case.

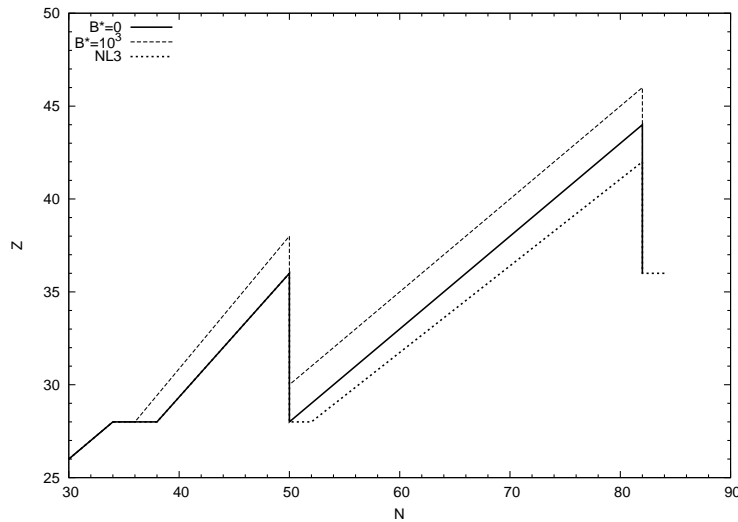


Figure 2. Proton number is shown as a function of neutron number for different theoretical nuclear models with and without magnetic fields.

We obtain the sequence of equilibrium nuclei minimizing the Gibbs free energy per nucleon for $B = 0$ and $B = 10^{16}$ G. These results are obtained with and without the lattice energy correction. We compare our findings at $B_* = 10^3$ with those of zero field case and find that some new equilibrium nuclei such as $^{88}_{38}\text{Sr}$ and $^{128}_{46}\text{Pd}$ appear and some nuclei such as $^{66}_{28}\text{Ni}$ and $^{78}_{28}\text{Ni}$ disappear in the presence of the magnetic field. Further we note that the maximum density (ρ_{max}) upto which an equilibrium nucleus can exist, increases as the field strength increases. As a result the neutron drip point is shifted from 4.34×10^{11} g/cm³ in zero field to 4.92×10^{11} g/cm³ in the strong magnetic field. The lattice energy correction influences our results in strong magnetic fields. It is worth mentioning here that our results are different from those of earlier calculation [5] because we have adopted most recent experimental and theoretical nuclear mass tables. For $B = 0$, we note that $^{122}_{38}\text{Sr}$ which was present in the previous calculation [5] is absent in our case. A comparison of our results at zero field with those of Lai and Shapiro [5] shows that equilibrium nuclei have higher ρ_{max} in the former case. Further we performed our calculation at higher magnetic fields than the previous calculation [5].

Figure 2 displays the proton number as a function of neutron number. We compare sequences of equilibrium nuclei calculated with experimental nuclear masses from atomic mass table of Audi, Wapstra and Thibault [10] and theoretical nuclear mass models for those nuclei which are not listed in the experimental mass table. We use the theoretical model of Möller et al. [11] and relativistic mean field model with NL3 set [12, 13]. It is evident from the figure that

for zero magnetic field our calculation of equilibrium nuclei initially agrees with those of the relativistic model calculation because nuclear masses are obtained from the experimental mass table. However, both calculations for zero magnetic field differ considerably beyond $N=50$ due to differences in theoretical mass tables used here.

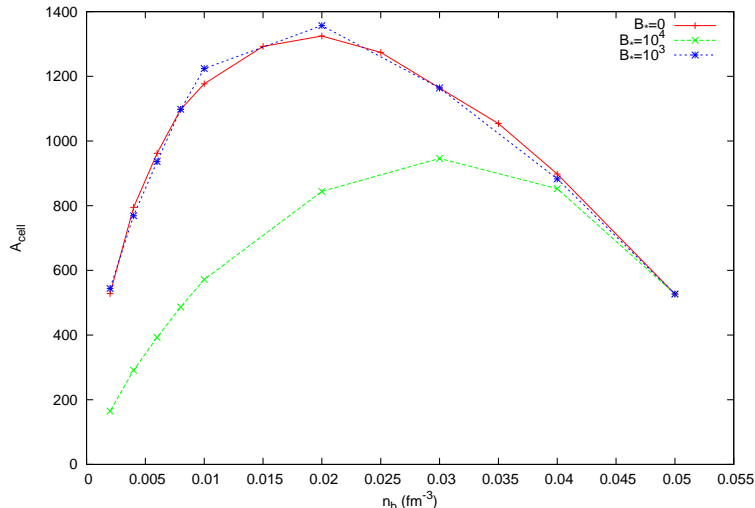


Figure 3. Mass number is displayed as a function of average baryon density.

3. Inner Crust in Magnetic Fields

Next we investigate the stability of nuclei in the inner crust in the presence of strong magnetic fields using the Thomas-Fermi model. In this case nuclei are immersed in a neutron gas as well as in a uniform background of electrons. The coexistence of liquid and gas phases of nuclear matter is considered here. In the inner crust, nuclei are also arranged in a lattice. The Wigner-Seitz approximation is adopted in this calculation. However, the spherical cell in which protons and neutrons coexist does not define a nucleus. The nucleus is realised after subtraction of the gas part from the cell. This is done following the procedure of Bonche, Levit and Vautherin [14]. In this case, the density profile of liquid plus gas system and that of the gas are obtained in a self-consistent way and the liquid part which ultimately becomes the nucleus, is calculated as the difference of two solutions. We assume β -equilibrium $\mu_n = \mu_p + \mu_e$. Electrons are affected by quantizing magnetic fields like the outer crust. The proton density in the cell is affected by magnetic fields through the charge neutrality condition. We minimise the free energy which is a function of average baryon density (n_b) and proton fraction (Y_p), in the cell

$$\mathcal{F}(n_b, Y_p) = \int [\mathcal{H} + \varepsilon_c + \varepsilon_e] d\mathbf{r} , \quad (13)$$

where \mathcal{H} is nuclear energy density functional, ε_c is the coulomb energy density and ε_e is the energy density of electrons. The nuclear energy density is calculated using SKM* nucleon-nucleon interaction [15]. We perform this calculation for temperature $T=0$.

Now we present our results related to the inner crust. We fix the average baryon density n_b and achieve the β -equilibrium changing the proton fraction Y_p . Next we find the minimum of the free energy varying the cell size. We perform this calculation for $B = 0$ and $B_* = 10^3, 10^4$. We do not find any appreciable difference in our results for $B = 0$ and $B_* = 10^3$. However, the cell size is appreciably reduced in case of $B_* = 10^4$. In this case only zeroth Landau level is

populated below the density 0.06 fm^{-3} . This leads to the large enhancement of proton fraction in the cell through the Landau quantization of electrons. Above this density, electrons populate finite number of Landau levels and the cell size and proton fraction in the magnetic field case become equal to those of the zero field. The size of the cell as well as proton fraction decrease as density increases.

Figure 3 displays mass number (A_{cell}) of nuclear cluster as a function of average baryon density for $B = 0$ and $B_* = 10^3, 10^4$. These are obtained after minimising the free energy at each density point. It is noted that at any density point the mass number of the nuclear cluster in magnetic field $B_* = 10^4$ is lower than the corresponding nuclear cluster at zero magnetic field. Further we obtain the liquid part of the cell after subtraction of the gas part and define this as a nucleus. We find nuclei with larger mass number in the presence of a strong magnetic field $\sim 10^{17} \text{ G}$ compared with the zero field case. Further nuclei are more bound in strong magnetic fields than the corresponding nuclei in $B = 0$ at the same baryon density.

4. Summary and Conclusions

We have revisited the BPS model of outer crust in the presence of strong magnetic fields $\sim 10^{16} \text{ G}$ or more using the recent experimental mass table. Further we have included the correction in the lattice energy due to the finite size of a nucleus. For zero magnetic field case, it is noted that maximum densities for heavier nuclei in this calculation are higher than those of the previous calculation [5]. In the presence of a strong magnetic field, there are modifications in the sequence of nuclei compared with the zero field case. We have further investigated the inner crust in the presence of strong magnetic fields. For $B = 10^{17} \text{ G}$, it has been observed that proton fraction is enhanced at lower densities and mass numbers of nuclear clusters after subtracting the gas part are higher than those of the zero field. It would be worth investigating the implications of our results for the transport properties such as thermal and electrical conductivities and shear viscosity of the crust in magnetars.

5. Acknowledgment

We acknowledge the support of the Alexander von Humboldt Foundation under the Research Group Linkage Programme.

- [1] Lai D 2001 *Rev. Mod. Phys.* **73** 629
- [2] Vasisht G and Gotthelf E V 1997 *Astrophys. J* **486** L129
- [3] Kouvelouotou C et al. 1998 *Nature* **393** 235;
Kouvelouotou C et al. 1999 *Astrophys. J.* **510** L115
- [4] Thompson C and Duncan R C 1993 *Astrophys. J.* **408** 194;
Thompson C and Duncan R C 1996 *Astrophys. J.* **473** 322
- [5] Lai D and Shapiro S L 1991 *Astrophys. J.* **383** 745
- [6] Chakraborty S, Bandyopadhyay D and Pal S 1997 *Phys. Rev. Lett.* **78** 2898
- [7] Baym G, Pethick C and Sutherland P 1971 *Astrophys. J.* **170** 299
- [8] Baym G, Bethe H A, and Pethick C J 1971 *Nucl. Phys. A* **175** 225
- [9] Negele J W and Vautherin D 1973 *Nucl. Phys. A* **207** 298
- [10] Audi G, Wapstra A H and Thibault C 2003 *Nucl. Phys. A* **729** 337
- [11] Moller P, Nix J R, Myers W D and Swiatecki W J 1995 *At. Data Nucl. Data Tables* **59** 185
- [12] Ruster S B, Hempel M and Schaffner-Bielich J B 2006 *Phys. Rev. C* **73** 035804
- [13] Bender M et al. 1999 *Phys. Rev. C* **60** 034304
- [14] Bonche P, Levit S and Vautherin D 1985 *Nucl. Phys. A* **436** 265
- [15] Sil T et al. 2002 *Phys. Rev. C* **66** 045803